

# Lesion Segmentation in Dermoscopy Images Using Particle Swarm Optimization and Markov Random Field

Khalid Eltayef, Yongmin Li and Xiaohui Liu

*Department of Computer Science, Brunel University, Uxbridge, UB8 3PH, UK  
Khalid.Eltayef@Brunel.ac.uk, Yongmin.Li@Brunel.ac.uk, XiaoHui.Liu@brunel.ac.uk*

**Abstract**—Malignant melanoma is one of the most rapidly increasing cancers globally and it is the most dangerous form of human skin cancer. Dermoscopy is one of the major imaging modalities used in the diagnosis of melanoma. Early detection of melanoma can be helpful and usually curable. Due to the difficulty for dermatologists in the interpretation of dermoscopy images, Computer Aided Diagnosis systems can be very helpful to facilitate the early detection. The automated detection of the lesion borders is one of the most important steps in dermoscopic image analysis. In this paper, we present a fully automated method for melanoma border detection using image processing techniques. The hair and several noises are detected and removed by applying a bank of directional filters and Image Inpainting method respectively. A hybrid method is developed by combining Particle Swarm Optimization and Markov Random Field methods, in order to delineate the border of the lesion area in the images. The method was tested on a dataset of 200 dermoscopic images, and the experimental results show that our method is superior in terms of the accuracy of drawing the lesion borders compared to alternative methods.

**Keywords**-Markov Random Field, Particle Swarm Optimization, image segmentation, dermoscopy images, melanoma, skin lesion detection.

## I. INTRODUCTION

Malignant melanoma is considered as one of the most fatal forms of skin cancer, which led to increase the mortality rate. In the last few decades, the incidence of melanoma has increased significantly, especially among white-skinned people who are exposed to the sun. For instance, in North America melanoma became the fifth common cancer among males and the sixth common cancer among females, while the fourth most common in Australia [1].

Dermoscopy is considered as one of the major imaging modalities which can be used for detecting and diagnosing melanoma. It is a widely used technique by dermatologists and helps them to identify and diagnose melanoma in early stage. It allows the identification of several features such as dots, streaks, bluewhite areas and pigmented networks by making them more visible [2] [3], since one or two features alone cannot identify malignancy in the lesion. By using dermoscopy images, the dermatologists became more confident in distinguishing the lesion area. In melanoma de-

tection, the dermatologists utilize the ABCD rule to analyze four parameters (Asymmetry, Border, Colors and Diameter) and identify the lesion area. In addition, 7-point checklist criteria also used for the same purpose [1] [4] [5] [6]. Due to the existence of hair and reflection artifacts on the images, also many melanoma borders are often invisible or fuzzy which makes visual identification very difficult for dermatologists, and the interpretation of the images is time consuming and subjective. The Computer Aided Diagnosis (CAD) became essential and necessary, in order to get rid of all these issues and assist the specialists and physicians to interpret the image clearly and get the right decision for their diagnosis. CAD systems have been proposed by many research groups to identify various structures in medical images. Depending on medical knowledge, CAD systems try to mimic the performance of dermatologists for the detection of the lesion area [7]. Integrating dermoscopy techniques with CAD techniques is a very important research field.

The standard approach in dermoscopic image analysis often comprises of four phases: artifacts detected and removed, lesion segmentation, feature extraction and lesion classification. The image segmentation stage is the most important step since the accuracy of the subsequent steps depends on its performance. Consequently, all of the following stages will be affected and wrong diagnosis will be obtained. However, dermoscopic image segmentation and delineation of the border of the lesions is a challenging task, because of the low contrast between the lesion area and the healthy skin. Moreover, several artifacts such as air bubbles, oil, lightening reflection and dark hair present in almost all images.

This paper presents a novel method for melanoma detection on dermoscopy images. First, the image is pre-processed to remove the noise and enhance its quality. Second, Particle Swarm Optimization (PSO) and Markov Random Field (MRF) are combined to segment the lesion from images. Upon comparison, the proposed approach provides high performance in achieving automatic image segmentation on dermoscopic images. The rest of the paper is organized as follows. The previous methods are reviewed in Section II. An overview of the MRF and PSO methods are described in Section III. The details of the proposed method are described in Sections IV. The details of experiments and result analysis

are discussed in Section V. Finally, conclusions are drawn in Section VI.

## II. PREVIOUS WORK

Several segmentation methods have been developed to locate and detect the skin lesions in images automatically, a few of them for the conventional macroscopic images and the others for the dermoscopy images. In this section, we review several methods applied on dermoscopy images to extract the lesion area.

Jaworek et al. [8] used region-growing method to detect the lesion border in dermoscopy images. A novel automatic segmentation approach is proposed by Garnavi et al. [9]. The authors used color space analysis and clustering based on histogram thresholding to find out the optimal color channel for segmentation of skin lesions. Fuzzy c-means (FCM) thresholding technique is used to locate and segment the lesions from dermoscopy images [10], [11]. An automatic adaptive threshold (AT) is used by Silveira et al [7]. The extraction of color and texture descriptors from dermoscopy images were used to feed the deep Convolutional Neural Network (CNN), that to distinguish between lesions and normal skin Jafari et al. [12]. Hwang et al [13] used Gabor filters approach to extract several texture features from dermoscopy images and applied g-means clustering method to segment the lesion area. Dermoscopy image segmentation based on texture distinctiveness (TD) is proposed by Jeffrey et al [14]. Their proposed method tried to capture the dissimilarity between different texture distributions based on TD metric. Barata et al. [15] proposed two systems for melanoma detection in dermoscopy images. The texture and color features have been used based on local and global features. Histogram computation, peak detection and threshold estimation were implemented to get adaptive threshold and segment the lesion.

## III. OVERVIEW OF THE MRF AND PSO METHODS

### A. The MRF Method

As a statistical method, the MRF provides a tool for Bayesian modelling using spatial continuity and has been widely used in image segmentation with numerous applications [16]–[18]. It is usually based on local calculation of probability and potential functions. The pixels of the image are indexed by a rectangular patch  $S$  and each image pixel  $s$  is characterized by the gray level  $y_s$  from the set  $y = \{y_s : s \in S\}$ . The labelling process consists of accurately labelling each image pixel  $s \in S$  with a class label representing the pattern class in the image. A label set is defined as  $\Lambda = 1, 2, \dots, C$  where  $C$  is the number of classes. A labelling is indicated by  $x = x_s : x_s \in \Lambda, s \in S$  where  $x_s = l$  denotes that the class label  $l$  is assigned to the pixel  $s$ . The goal is to find the labelling  $\hat{x}$  of the image, which maximizes  $P(x|y)$  based on the Bayes decision theorem.

### B. The PSO Method

The original PSO method proposed by Eberhart and Kennedy [19] is a computational optimization method based on swarm intelligence theory. It is initialized with a group of random particles in order to find the optimal solution through the search space, each particle represents a candidate solution of the problem based on a fitness function. In the PSO approach, the whole swarm is modelled as multidimensional space  $S$ , therefore, each particle  $P_i = \{F_i, V_i\}$  has two components: position  $F_i$  and velocity  $V_i$ . The best previously visited position of particle  $i$  is denoted as its individual best position while the best position of all these individual bests is denoted as the global best position. In the beginning, the position and the velocity of each particle (solution of the problem) are initialized randomly. Then, the problem is being optimized by flying each particle through the search space and updating its individual best position and global best position. Therefore, the performance of each particle is evaluated using a fitness function. This process is repeated until a stopping criterion is met. The stopping criterion could be that all particles positions do not change any more than a certain threshold, or the maximum number of iterations is met. At each step, the velocity and the position of particle  $f_i$  are updated using (1) and (2), respectively.

$$v_i = w \times v_i + c_1 \times r_1 \times (fb_i - f_i) + c_2 \times r_2 \times (G - f_i) \quad (1)$$

$$f_i = f_i + v_i \quad (2)$$

where  $w$  is the inertia weight which controls the interaction power between the particles,  $v_i$  is the current velocity and  $f_i$ ,  $fb_i$  and  $G$  are current position of the particle, the best position which particle has achieved so far and the location of overall best value respectively. The  $r_1$  and  $r_2$  are random values generated in the range between 0 and 1. The positive values  $c_1$  and  $c_2$  are constants referring to the acceleration coefficients in order to guide particles into good directions and control the maximum step size.

## IV. THE PROPOSED METHOD

In the pre-processing stage, the image enhancement is carried out by detecting hairs and reflection artifacts. The Image Inpainting method is applied to remove the pixels which indicate the hairs and reflection artifacts mask. The second step of the proposed method is to delineate the border of the lesion area, which is achieved by combining PSO with MRF method. Full details of individual steps are described as follows.

### A. Dermoscopic Image Preprocessing

Generally, in image processing techniques the pre-processing stage is the first process that can be executed, since digital images usually contain noise and reflection illumination, which in turn affect the subsequent stages. In

dermoscopy images, this step is essential and mandatory since the hairs covering the lesion area and many reflection artifacts must be detected and removed. This section illustrates an image processing approach to detect and extract these kind of noise from dermoscopy images. The original RGB images are separated to three color components then the blue component is selected, as it has been experimentally proven to provide the best discrimination in most dermoscopy images [7].

1) *Reflection Detection*: In dermoscopy images, reflection artifacts and air bubbles indicate the noise which must be detected and removed, since its impact on subsequent stages is very high. To detect these kinds of noise, a simple thresholding method is carried out. Every single pixel  $(x, y)$  can be detected and classified as a reflection artifact if its intensity value is higher than threshold  $T_{R1}$  and if its intensity value minus the average intensity  $I_{avg}(x, y)$  of its surrounding neighborhood is higher than threshold  $T_{R2}$ , i.e.

$$\{I(x, y) > T_{R1}\} \text{ and } \{(I(x, y) - I_{avg}(x, y)) > T_{R2}\}. \quad (3)$$

where  $I$  is the image,  $I_{avg}(x, y)$  is the average intensity value in a local neighborhood of the selected pixel which is computed using a local mean filter with dimensions  $11 \times 11$  and  $T_{R1}=0.7$ ,  $T_{R2}=0.098$ .

2) *Hair Detection and Inpainting*: Most of dermoscopy images contain hairs, which in turn could affect the outer borders of the lesion area, since their shapes are similar. Thus, this leads to wrong detection of the lesion or make the borders invisible. Consequently, for effective segmentation, hairs must be detected and removed. Based on our knowledge, median filter, adaptive threshold and morphological operations such as Top Hat filter (Opening and Closing image) were widely used for this purpose [1] [5] [9] [10]. To do so, the directional Gabor filters are applied using a bank of 64 directional filters. Thus, at each stage the images are filtered by each directional filter with different parameters set as:  $\sigma_{x1} = 20$ ,  $\sigma_{y1} = 6$ ,  $\sigma_{x2} = 20$  and  $\sigma_{y2} = 1.5$ . Then, the difference of Gaussians is implemented, followed by finding the local maximum at each pixel location. Therefore, the Threshold method is used to classify each image pixel as either hair or background. Details of the method can be obtained from [20] [21]. The outcomes of the previous step are clean hair masks which will be used to implement the Image Inpainting method. The binary masks are multiplied by gray scale images. This step leads to appearance of gaps which indicate the unknown regions in the images. Therefore, these regions could be filled by propagating the information from surrounding neighbourhood (known regions). Patch priorities (data term and confidence term) are computed in the borders of the unknown regions based on their neighbours. The patch with the highest priority is filled out with data extracted from the source region, and then the patch priorities are updated. This process continues till no more gaps exist. A detailed explanation of the method



Figure 1. Example of hair detection process and inpainting images: original (first column), hair detection (second column) and inpainted image (third column).

can be found in [22]. The final images obtained are clean which will be used in the subsequent step. One example can be seen in Fig. 1.

### B. Skin Lesion Segmentation

Image segmentation is the process of adequately separating pixels into few groups, whose pixels share similar characteristics, such as texture, color, and shape. Indeed, the performance of segmentation should be fast and accurate, since all the subsequent steps such as: feature extraction, feature selection and classification phase are dependent on its performance. In dermoscopy images, the segmentation stage is one of the most important and challenging step, due to several reasons such as: the lesions have large variations in size and color, low contrast between the lesion area and surrounding healthy skin as well as, presence of the hairs with several artifacts as mentioned earlier.

The main aim of our approach is to build an efficient, robust and automatic segmentation tool for melanoma lesion detection. Image segmentation phase is implemented in order to separate the lesion area from the healthy skin. Useful results can be acquired by applying appropriate segmentation technique. For this reason, the PSO and the MRF methods were combined to perform the final segmentation of the images by minimizing the energy function.

The image segmentation is formulated as an optimization problem of the energy function with the MRF method. For this, we use the PSO method to perform the initial labelling. The underlying idea of our approach is a cooperative search of the best class label for each pixel in the image using a population of artificial particles. Each particle assigns pixels to a class iteratively based on fitness function. In the beginning, the number of particles is determined, and then the position value of each particle is randomly set within the boundaries of the search space, while the velocity of each particle is set to zero. The search space will rely on the maximum intensity value  $L$ , which means the number of particles are distributed randomly between 0 and 255. One particle in the swarm represents one solution for clustering the image based on fitness function. Therefore, the whole swarm represents a number of candidate clustering solutions for the whole image. In each step of the proposed algorithm, each particle compares its current fitness value with the value of its own  $Pbest$  solution as well as, the fitness value of the whole swarm  $Gbest$  solution. The fitness function is

defined as the between-class variance  $\sigma_b^2$  of the intensity distributions of the image [23] by:

$$\sigma_b^2 = \sum_{j=1}^n w_j (\mu_j - \mu_t)^2 \quad (4)$$

where  $j$  represents a specific class in such a way that  $\mu_j$  and  $w_j$  are the average and the probability of occurrence of class  $j$ , respectively. The probabilities of occurrence  $w_j$  of class  $D_1, \dots, D_n$  are given by:

$$w_j = \sum_{i=1}^{t_j} p_i, j = 1 \quad (5)$$

where  $p_i$  is the probability of occurrence of each pixel in the image which can be obtained by

$$p_i = \frac{h_i}{N}, \sum_{i=1}^N p_i = 1 \quad (6)$$

where  $i$  represents intensity level, *i.e.*,  $0 \leq i \leq L-1$ ,  $N$  represent the total number of the pixels in the image and  $h_i$  refers to image histogram.

And the average of each class  $\mu_j$  can be calculated as:

$$\mu_j = \sum_{i=1}^{t_j} \frac{ip_i}{w_j}, j = 1 \quad (7)$$

where  $ip_i$  presents the total mean (combined mean) and can be obtained by:

$$\mu_t = \sum_{i=1}^L ip_i \quad (8)$$

In other words, the segmentation problem is reduced to an optimization problem to search for the optimal threshold value by maximizing the fitness function. Higher fitness means more probability of this particle being successful.

$$ft = \max \sigma_b^2(t) \quad (9)$$

Therefore, the optimal threshold value can be used for dividing the image into 2 classes, foreground and background. By this process, we can get the membership value easily for each pixel in the image by:

$$g(x, y) = \begin{cases} 1, & \text{if } f(x, y) > T \\ 0, & \text{if } f(x, y) \leq T \end{cases} \quad (10)$$

The main drawback with the PSO approach is that it deals with each pixel individually by using its intensity value, In order to address this issue and improve the performance of PSO method, an additional local search is performed for each segmented image by combining it with MRF method. The main aim of using the MRF to perform image segmentation is minimizing the energy function or maximizing the probability of pixel allocation to a cluster by using Maximum A Post Priority (MAP) [16]. According to the MAP estimate and the Hammersley-Clifford theorem

[24] with assumption of existence of Gaussian noise in the images, the energy function can written as

$$U(x) = \left[ \sum_{s \in S} \frac{(y_s - \mu_{xs})^2}{2\sigma_{xs}^2} + \sum_{s \in S} \log(\sigma_{xs}) + \sum_{c \in C} V_c(x) \right] \quad (11)$$

In our algorithm, we used the membership value instead of the conditional probability in order to assign each image pixel properly and refine the segmented image. Equation (12) is used to calculate the conditional probability.

$$V_c(y_i|x_j) = g(x, y) \quad (12)$$

The Iterated Conditional Modes (ICM) method is widely used for the MRF applications, which achieves optimal labelling with minimum energy. Actually, ICM is an iterated algorithm, which maximizes local conditional probabilities by propagating messages along nodes in the MRF. Therefore, we use it to obtain optimized clusters. In our method we assume that one pixel has 8-neighbors. Therefore, the second order clique potential is defined on pairs of neighbouring pixels:

$$V_c(xi, xj) = (1 - i_{xi, xj}) \quad (13)$$

where  $i_{xi, xj} = 0$  if  $xi \neq xj$  and 1 if  $xi = xj$ . Therefore, the energy function is defined as sum of conditional probability and the second order energies as in (14).

$$U(X) = \sum_{i \in S} V_c(y_i|x_j) + \sum_{j \in S} \sum_{N_i} V_c(xi, xj) \quad (14)$$

By applying the PSO approach, each pixel in the image is labeled to a cluster based on the highest fitness function. Thus, to perform the local search and refine the segmented image, we integrate the PSO with the MRF approach. Accordingly, all pixels will be labeled again to different classes by getting the minimum cost (14). This process continues until stopping criterion is met or no further change occurs between clusters. Finally, due to presence of several holes inside the segmented lesion as well as few outlier pixels in the background, Morphological Operations were used to fill in and remove these pixels respectively.

## V. RESULTS AND DISCUSSIONS

The proposed method was tested on a publicly available database PH2 [25] which provides 200 dermoscopy images. Four different criteria have been selected to evaluate the performance of the segmentation results: sensitivity (SE), specificity (SP), accuracy (AC) and the Dice similarity coefficient (DSC). Segmentation of the skin lesion was implemented using PSO, Fuzzy C-Means (FCM) [26] and the proposed method respectively. Thus, the comparison of these three methods was performed with the lesions acquired by expert dermatologist, so as to evaluate the performance of the proposed method.

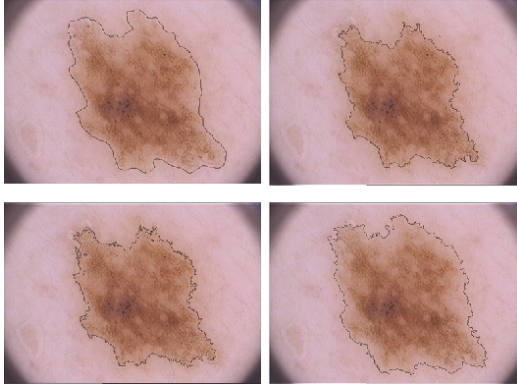


Figure 2. Results of lesion detection: the ground truth (top left), PSO (top right), FCM (bottom left) and the proposed method (bottom right).

Examples of manual segmentation by radiologists together with the results by three methods of skin lesion segmentation are shown in Fig. 2. The ground-truth is shown in the top left image, and results obtained using the PSO, FCM and the proposed method are in the top right, bottom left and bottom right images respectively. In general, the proposed method has the best performance in terms of the accuracy. For instance, as we can see in Fig. 2, the image in the top right (PSO method) did not succeed in delineating the entire lesion, with part of the lesion misclassified as a healthy skin (background). Also the detected edge is not close to the actual boundary of the lesion which leads to misclassification. The same happened when the FCM method was applied, as we can see in the bottom left image. The result from the proposed method shows that the detected edge is close to the real boundary of the skin lesion and almost the whole lesion was detected and delineated.

In addition to the visual observations, we have carried out a quantitative evaluation by comparing the performance of our method against a selection of seven alternative methods namely J-image segmentation (JSEG) [27], Statistical Region Merging (SRM) [28], Otsu [29], Level Set [30], Automatic Skin Lesion Method (ASLM) [31], PSO [23] and FCM [26]. The experimental results on the same dataset of 200 dermoscopy images are presented in Table I. For all the four metrics, the proposed method achieved the best segmentation performance.

## VI. CONCLUSIONS

A fully automatic lesion segmentation method from dermoscopy images is presented in this paper. The Gabor filter and image inpainting methods are carried out to detect and remove the hairs and other artifacts from the images. Lesion regions are segmented by integrating the PSO and the MRF methods. In each iteration, the segmented images obtained by using PSO method are combined with the MRF method in order to do local search and minimize the energy

Table I  
SEGMENTATION PERFORMANCE ON THE COMPLETE DATASET  
SE-SENSITIVITY, SP-SPECIFICITY, AC-ACCURACY AND DSC-DICE  
SIMILARITY COEFFICIENT.

Method	SE	SP	AC	DSC
PSO [23]	0.7826	0.9909	0.9187	0.8481
FCM [26]	0.8880	0.9517	0.9339	0.9040
JSEG [27]	0.7108	0.9714	0.8947	0.7554
SRM [28]	0.1035	0.8757	0.6766	0.1218
Otsu [29]	0.5221	0.7064	0.6518	0.4293
Level Set [30]	0.7188	0.8003	0.7842	0.6456
ASLM [31]	0.8024	0.9722	0.8966	0.8257
Proposed Method	<b>0.9388</b>	<b>0.9758</b>	<b>0.9474</b>	<b>0.9231</b>

function. Therefore, each pixel is reassigned to a different class depending on its neighbourhood pixels.

The proposed method achieved approximately 95.0% accuracy, 94.0% sensitivity, and 98.0% specificity on a public dataset of 200 images. A comparison against a selection of seven alternative methods shows that the proposed method performs the best in terms of sensitivity, specificity, accuracy and the Dice similarity coefficient. All the above indicate that this approach is able to deal with light reflection, the presence of hair and other artifacts such as air/oil bubbles, and to provide high accuracy of skin lesion detection. Moreover, it has a great potential to identify the borders of the lesions and is able to support the clinical diagnosis.

## ACKNOWLEDGEMENT

The dataset used in this study was obtained from [25]. The authors would like to thank Catarina Barata for sharing.

## REFERENCES

- [1] G. Capdehourat, A. Corez, A. Bazzano, R. Alonso, and P. Musé, "Toward a combined tool to assist dermatologists in melanoma detection from dermoscopic images of pigmented skin lesions," *Pattern Recognition Letters*, vol. 32, no. 16, pp. 2187–2196, 2011.
- [2] S. Suer, S. Kockara, and M. Mete, "An improved border detection in dermoscopy images for density based clustering," *BMC bioinformatics*, vol. 12, no. 10, p. S12, 2011.
- [3] M. E. Celebi, H. Iyatomi, G. Schaefer, and W. V. Stoecker, "Lesion border detection in dermoscopy images," *Computerized medical imaging and graphics*, vol. 33, no. 2, pp. 148–153, 2009.
- [4] A. G. Isasi, B. G. Zapirain, and A. M. Zorrilla, "Melanomas non-invasive diagnosis application based on the abcd rule and pattern recognition image processing algorithms," *Computers in Biology and Medicine*, vol. 41, no. 9, pp. 742–755, 2011.
- [5] D. Ruiz, V. Berenguer, A. Soriano, and B. SáNchez, "A decision support system for the diagnosis of melanoma: A comparative approach," *Expert Systems with Applications*, vol. 38, no. 12, pp. 15 217–15 223, 2011.

- [6] G. Argenziano, C. Catricalà, M. Ardigo, P. Buccini, P. De Simone, L. Eibenschutz, A. Ferrari, G. Mariani, V. Silipo, I. Sperduti *et al.*, “Seven-point checklist of dermoscopy revisited,” *British Journal of Dermatology*, vol. 164, no. 4, pp. 785–790, 2011.
- [7] M. Silveira, J. C. Nascimento, J. S. Marques, A. R. Marçal, T. Mendonça, S. Yamauchi, J. Maeda, and J. Rozeira, “Comparison of segmentation methods for melanoma diagnosis in dermoscopy images,” *IEEE Journal of Selected Topics in Signal Processing*, vol. 3, no. 1, pp. 35–45, 2009.
- [8] J. Jaworek-Korjakowska and R. Tadeusiewicz, “Determination of border irregularity in dermoscopic color images of pigmented skin lesions,” in *Engineering in Medicine and Biology Society (EMBC), 2014 36th Annual International Conference of the IEEE*. IEEE, 2014, pp. 6459–6462.
- [9] R. Garnavi, M. Aldeen, M. E. Celebi, A. Bhuiyan, C. Dolianitis, and G. Varigos, “Automatic segmentation of dermoscopy images using histogram thresholding on optimal color channels,” *International Journal of Medicine and Medical Sciences*, vol. 1, no. 2, pp. 126–134, 2010.
- [10] S. Sookpotharom, “Border detection of skin lesion images based on fuzzy c-means thresholding,” in *Genetic and Evolutionary Computing, 2009. WGECC’09. 3rd International Conference on*. IEEE, 2009, pp. 777–780.
- [11] K. Eltayef, Y. Li, and X. Liu, “Detection of melanoma skin cancer in dermoscopy images,” in *Journal of Physics: Conference Series*, vol. 787, no. 1. IOP Publishing, 2017.
- [12] M. Jafari, N. Karimi, E. Nasr-Esfahani, S. Samavi, S. Soroushmehr, K. Ward, and K. Najarian, “Skin lesion segmentation in clinical images using deep learning,” in *Pattern Recognition (ICPR), 2016 23rd International Conference on*, 2016.
- [13] S. Hwang and M. E. Celebi, “Texture segmentation of dermoscopy images using gabor filters and g-means clustering,” in *IPCV*, 2010, pp. 882–886.
- [14] J. Glaister, A. Wong, and D. A. Clausi, “Segmentation of skin lesions from digital images using joint statistical texture distinctiveness,” *IEEE transactions on biomedical engineering*, vol. 61, no. 4, pp. 1220–1230, 2014.
- [15] C. Barata, M. Ruela, M. Francisco, T. Mendonça, and J. S. Marques, “Two systems for the detection of melanomas in dermoscopy images using texture and color features,” *IEEE Systems Journal*, vol. 8, no. 3, pp. 965–979, 2014.
- [16] S. Geman and D. Geman, “Stochastic relaxation, gibbs distributions, and the bayesian restoration of images,” *IEEE Transactions on pattern analysis and machine intelligence*, no. 6, pp. 721–741, 1984.
- [17] A. Salazar-Gonzalez, Y. Li, and D. Kaba, “MRF reconstruction of retinal images for the optic disc segmentation,” in *International Conference on Health Information Science*. Springer, 2012, pp. 88–99.
- [18] A. Salazar-Gonzalez, D. Kaba, Y. Li, and X. Liu, “Segmentation of the blood vessels and optic disk in retinal images,” *IEEE journal of biomedical and health informatics*, vol. 18, no. 6, pp. 1874–1886, 2014.
- [19] R. Eberhart and J. Kennedy, “A new optimizer using particle swarm theory,” in *Micro Machine and Human Science, 1995. MHS’95., Proceedings of the Sixth International Symposium on*. IEEE, 1995, pp. 39–43.
- [20] K. Eltayef, Y. Li, and X. Liu, “Detection of pigment networks in dermoscopy images,” in *Journal of Physics: Conference Series*, vol. 787, no. 1. IOP Publishing, 2017.
- [21] C. Barata, J. S. Marques, and J. Rozeira, “A system for the detection of pigment network in dermoscopy images using directional filters,” *IEEE transactions on biomedical engineering*, vol. 59, no. 10, pp. 2744–2754, 2012.
- [22] A. Criminisi, P. Perez, and K. Toyama, “Object removal by exemplar-based inpainting,” in *Computer Vision and Pattern Recognition, 2003. Proceedings. 2003 IEEE Computer Society Conference on*, vol. 2. IEEE, 2003, pp. II–II.
- [23] P. Ghamisi, M. S. Couceiro, J. A. Benediktsson, and N. M. Ferreira, “An efficient method for segmentation of images based on fractional calculus and natural selection,” *Expert Systems with Applications*, vol. 39, no. 16, pp. 12 407–12 417, 2012.
- [24] J. Besag, “On the statistical analysis of dirty pictures,” *Journal of the Royal Statistical Society. Series B (Methodological)*, pp. 259–302, 1986.
- [25] T. Mendonça, P. M. Ferreira, J. S. Marques, A. R. Marçal, and J. Rozeira, “Ph 2-a dermoscopic image database for research and benchmarking,” in *Engineering in Medicine and Biology Society (EMBC), 2013 35th Annual International Conference of the IEEE*. IEEE, 2013, pp. 5437–5440.
- [26] J. C. Bezdek, R. Ehrlich, and W. Full, “Fcm: The fuzzy c-means clustering algorithm,” *Computers & Geosciences*, vol. 10, no. 2-3, pp. 191–203, 1984.
- [27] Y. Deng and B. Manjunath, “Unsupervised segmentation of color-texture regions in images and video,” *IEEE transactions on pattern analysis and machine intelligence*, vol. 23, no. 8, pp. 800–810, 2001.
- [28] R. Nock and F. Nielsen, “Statistical region merging,” *IEEE Transactions on pattern analysis and machine intelligence*, vol. 26, no. 11, pp. 1452–1458, 2004.
- [29] N. Otsu, “A threshold selection method from gray-level histograms,” *Automatica*, vol. 11, no. 285-296, pp. 23–27, 1975.
- [30] R. Crandall, “Image segmentation using the chan–vese algorithm,” *Project report from ECE*, vol. 532, 2009.
- [31] A. Pennisi, D. D. Bloisi, D. Nardi, A. R. Giampetruzzi, C. Mondino, and A. Facchiano, “Skin lesion image segmentation using delaunay triangulation for melanoma detection,” *Computerized Medical Imaging and Graphics*, vol. 52, pp. 89–103, 2016.